Journal of the Brazilian Society of Mechanical Sciences and Engineering (2018) 40:503
https://doi.org/10.1007/s40430-018-1425-9

TECHNICAL PAPER

# Design and additive manufacturing of patient-specific cranial and pelvic bone implants from computed tomography data

**Yashwant Kumar Modi**[1] · **Sidharth Sanadhya**[1]

Received: 19 December 2017 / Accepted: 24 September 2018 / Published online: 3 October 2018


**Abstract**
Additive manufacturing processes are being increasingly explored by researchers around the world for a variety of medical applications, such as patient-specific models, implants, prosthetics, orthotics, drug delivery devices and tissue engineering scaffolds. The objective of this study is to obtain patient-specific models and implants from computed tomography (CT) scan data and validate the strength of implant using finite element analysis. For this purpose, CT scan data of two patients were obtained in digital imaging and communication in medicine (DICOM) file format. DICOM files were converted into computer-aided design models using open source image processing software DeVIDE and saved in stereolithography (STL) format. The STL files were cleaned and corrected in Materialise's Magics RP software. These models were loaded into 3D systems' Geomagic Freeform software to design the customized implants. Finite element analysis was performed to check the strength of cranium implant. Maximum von Mises stress and deformation were found well below the allowable limit of the material. Finally, physical models of cranium, pelvic bone and implant prototypes, namely cranial, ilium, pubic symphysis and ischium were manufactured in polyamide PA2200 on a selective laser sintering machine. A simulation-based surface roughness evaluation was also performed to assess the range of surface roughness values ($R_a$) of various implant prototypes. The $R_a$ values for implants were observed between 14.4 and 34.67 µm.

**Keywords** Additive manufacturing · Patient-specific implant · STL · CT scan image · DICOM

## 1 Introduction

The success of any reconstructive surgery depends on precise preoperative medical assessment and appropriate planning for the surgery. Preoperative assessment and planning become even more important, when it comes to placement of an artificial implant inside the patient's body. One of the biggest challenges before the surgeons today is to ensure that the implant fits the damaged site properly, does not cause any post-surgical trauma or fail to perform its intended function. Till date, majority of the implants are manufactured by using conventional manufacturing processes and do not completely fulfil the stringent requirements of a specific patient. Although, conventionally manufactured standard implants are available in various sizes to meet the requirements of a wide variety of patients; they need to be modified by bending or cutting preoperatively or intraoperatively, which may not only lead to development of residual stresses in implant but also lengthen the operation time [1, 2]. Moreover, in complex cases like craniofacial and maxillofacial surgeries, great deal of care is needed to avoid damage to certain nerves and blood vessels during surgery [3]. This complicacy prolongs the surgery time. In order to avoid such circumstances, recently, physicians and surgeons have started employing patient's anatomical models to facilitate diagnosis, pre-surgery planning and communication between colleagues and patients [4]. Surgeons may use these medical models to pre-plan the surgery procedures in variety of ways, such as visualization of the patient's anatomy before treatment or surgery, simulation of surgery procedure before intervention, manufacturing of customized implants or templates prior to surgery and to communicate and train the staff members involved in patient treatment [5–11].

Technical Editor: Fernando Antonio Forcellini.

✉ Yashwant Kumar Modi
yashwant.modi@juet.ac.in

[1] Mechanical Engineering Department, Jaypee University of Engineering and Technology, A - B Road, Raghogarh, Dist. Guna, Madhya Pradesh 473 226, India

Additive manufacturing, developed in mid-1980s paved the path for rapid fabrication of complex customized medical models, implants and prosthesis with good accuracy [12–18]. According to ASTM International, AM is a process of joining materials to make parts from 3D model data, usually layer upon layer as opposed to subtractive manufacturing and formative manufacturing methodologies. Application of AM in medical area is becoming more and more popular day by day, as now it has become possible to convert patient's CT, MRI (magnetic resonance imaging), USG (ultrasound sonography), CBCT (cone beam computed tomography) data or even point cloud data into a CAD model using medical image processing or reverse engineering software [19, 20]. Once the CAD model of the patient's damaged tissue is obtained, it can be used for variety of purposes, such as manufacturing of a physical model to study and planning the complex surgeries, designing customized implants, prosthetics/orthotics, tissue engineering scaffolds. [4, 12, 13, 21–28]. The CT/MRI data of a patient are usually obtained in DICOM format [12]. DICOM is an international de facto standard for exchange, storage and communication of digital medical images. A single DICOM file may contain several two-dimensional (2D) images of a particular body part. Various commercial or open source software packages may be employed to obtain a CAD model from DICOM data. This CAD model can be used to perform finite element (FE) analysis. The same CAD model can be converted into a faceted file format, such as STL, PLY (polygon file format) and VRML (virtual reality modeling language), compatible to AM processes [29–32]. Finally, the faceted file is uploaded on an AM machine to fabricate a physical part. The end-use implant or prosthetic can be fabricated via two routes namely, direct manufacturing of end-use part or indirect manufacturing via rapid tooling (RT) technique [33]. In former case, an implant is directly fabricated using a biocompatible ceramic, plastic or metallic material using AM process. In the latter case, a prototype of the implant is first fabricated via rapid prototyping (RP) process and further this prototype is used as a pattern to cast the final implant in a biocompatible material. The implant must be tested for possession of adequate mechanical, chemical and biological properties before it is placed inside the patient's body [2, 34].

Cranioplasty has its root back in seventeenth century when the first xenograft was obtained from canine bone to repair a cranial defect in a Russian man [35]. During last three decades, focus of researchers has been on developing optimal osteo-integration materials as well as on development of novel procedures and techniques for customizing implant model generation [4, 36–39]. Many new materials such as carbon-based polymers, calcium-based alloplasts, metallic implants and biological grafts are being explored in order to cover large cranial defects [4, 40–42]. Advent of novel data capturing, image processing and modelling software has made reverse engineering process more precise, faster and economic. A combination of modern software and RE technique can dramatically improve the surgical efficiency in reconstructive cranioplasty [43].

The objective of this study is to describe methodology to obtain patient-specific physical biomodels of damaged bones as well as to design and develop customized implants for them with the help of cranial and pelvic CT-scanned data obtained from two different patients. Patient-specific implants produced through this approach will fit in damaged site perfectly without needing any intraoperative modifications. This will reduce not only surgery and patient recovery time but also reduce the chances of implant failure in future as compared to conventional implants. Authors have used open source software DeVIDE as well as commercial software Magics RP and Geomagic freeform to carry out this study. However, the process may be made more cost-effective by using open source software such as Mesh Lab, Blender, FreeCAD. In order to access surface roughness of the fabricated implant prototypes, a simulation-based surface roughness evaluation is also presented at the end. Whole procedure to obtain 3D models and designing of implants from CT scan data has been explained in subsequent paragraphs in detail.

## 2 Methodology

For obtaining physical models of cranium, pelvic bone and various implants using patient-specific CT scan data involves many steps, such as identification of a patient, obtain CT scan data in DICOM format, converting DICOM image data in 3D STL and CAD models, and design and analysis of the customized implants and manufacturing of models and implants using AM. Methodology adapted by the authors to obtain implant prototypes is shown in Fig. 1.

### 2.1 To obtain CT/MRI data of a patient

This is the initial step towards manufacturing of a patient-specific physical biomodel. A patient is identified in collaboration with a doctor or a hospital. Now, CT scan or MRI data of the patient's defect site are obtained. CT/MRI data contain 2D images and are used to generate a 3D model of patient's specific bone/tissue. These images are required to be very precise and accurate; hence, a spiral scanning technique may be used which allows full volume scanning. Full volume scanning generates large number of slices and also allows adjusting size of pixels in each slice depending on the case. The CT or MRI data are now stored in DICOM format. For this study, authors obtained CT-scanned DICOM images of damaged pelvic bone and skull of two different

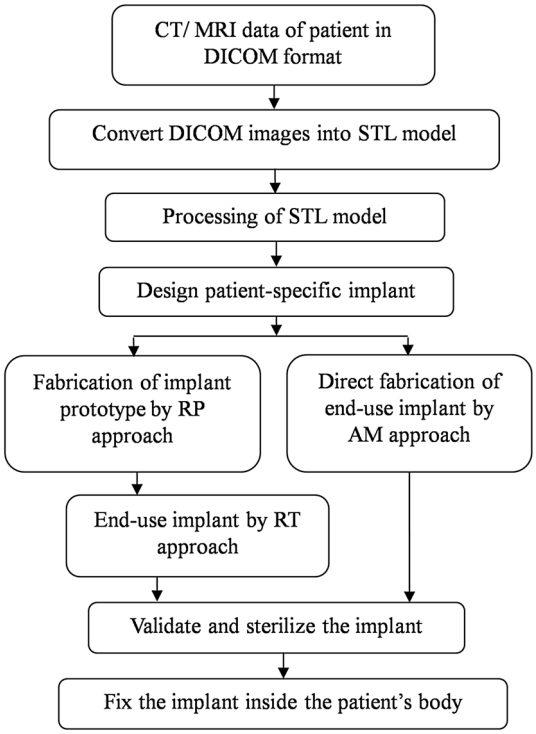


**Fig. 1** Methodology to fabricate patient-specific model/implant

patients (Age 37–42 years). Scanning was performed using SOMATOM Definition AS 64-slice CT scanner (Siemens Medical Systems, Erlangen, Germany) with the parameters: tube voltage 100 kV, tube current 120 mA and slice thickness 1.2 mm. The scanned data were saved in DICOM file format.

## 2.2 Conversion of DICOM images into STL model

For fabricating physical biomodel via additive manufacturing, we require a CAD model of the tissue/bone preferably in STL file format. The DICOM data obtained via CT/MRI machine contain only 2D images and need to be converted into a CAD model before inputting to AM machine. For this purpose, various proprietary (e.g. Geomagic Freeform, 3D Systems, USA; MIMICS, Materialise, Belgium; 3D Doctor, Able Software Corps, USA, Simpleware, Synopsys, USA) as well as open source (e.g. DeVIDE, Visualization Group; InVesalius, Brazil, Osirix, Switzerland) biomedical image processing software packages are available in market. These packages allow us to create and visualize 3D CAD model from the 2D images by performing image manipulation and segmentation. We also need to separate different tissues (soft and hard tissues/bones) in 2D images during the image manipulation. This is achieved through segmentation of the image. Segmentation is the separation of the structures, which

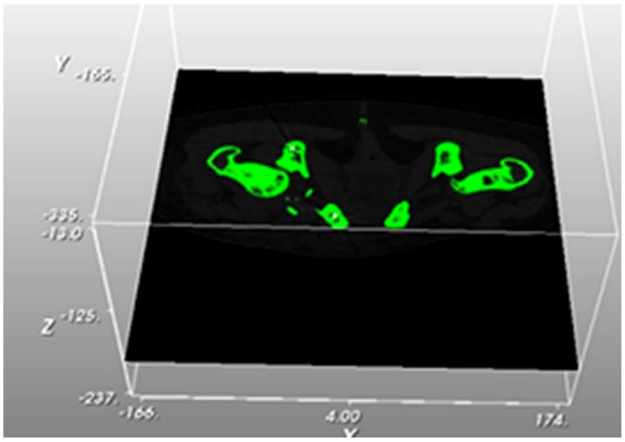


**Fig. 2** Pelvic bone after applying 'double threshold' and 'clean dvmr' module in DeVIDE

should be represented in the biomodel of the undesirable adjacent structures. There are various methods of image segmentation, such as region based, edge based, threshold, feature based. However, most of the software packages use the threshold method. This tool is based on the definition of a range of grey densities that expresses, for example, only pixels corresponding to the osseous tissue. Although it may seem to be a simple task, in practice, it is one of the salient points of the process. When this range is inappropriately determined, there may be a thickening or a thinning of the osseous structures of interest. They may even be deleted during the process, resulting in undesirable dimensional changes. A radiologist and a surgeon may prove very helpful in obtaining right region of interest, like separating bone from tissues, exclude anomalous structures, noise by right segmentation with a good resolution and optimum size of pixels. After segmentation, 3D virtual model of the desired tissue is obtained. This 3D biomodel is saved as an STL file by the biomedical software.

The DICOM file of pelvic bone chosen for this study contains a total of 355 slices. Authors used DeVIDE software to convert DICOM images into 3D STL model. The threshold technique was used to extract the bony part only. For this purpose, 'double threshold' module was used with upper threshold value as 3000 HU (Hounsfield unit) and the lower threshold value as 250 HU. The extracted surface was then cleaned up using the 'clean dvmr' module resulting in the dilation of the highlighted bone surface and removal of surface errors left by separation of the soft tissue as shown in Fig. 2. The surface irregularities were smoothed out using the 'Mesh smoother' module.

3D model obtained was saved as an STL file using 'stlwr' module as shown in Fig. 3. This STL file can be further processes and used as a base for implant designing process.

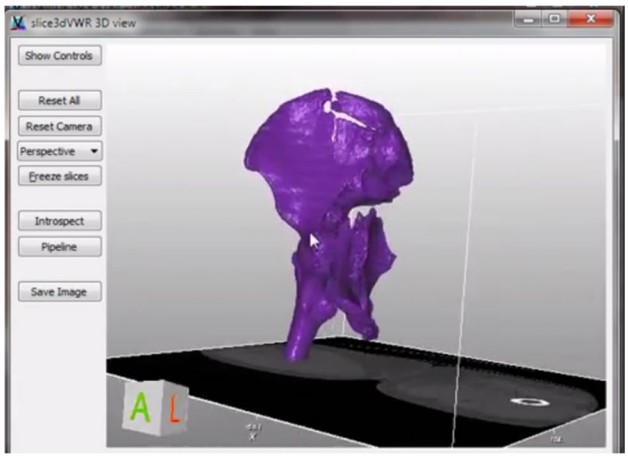


**Fig. 3** Screenshot of STL model of Pelvic bone in DeVIDE

## 2.3 Processing of STL model

The STL format converts the surface of the 3D biomodel into thousands of small triangular facets. This process of converting 3D model into faceted model is usually not perfect and involves inclusion of errors like flip normal or gapes between triangles. Software like Magics RP, Materialise, Belgium or Mesh Lab (open source software) may be employed to identify and fix such errors. These software also allow us to increase or decrease the number of triangles in the faceted model to adjust the surface quality of the model. Authors have used Magics RP software to perform pre-processing of the STL file obtained from the DeVIDE software. The number of triangles was increased to improve the surface quality of the models. Many errors like flip normal, open, overlapping and missing facets, convex boundary errors, common node were repaired using automatic repair facility. The final rectified STL model of the pelvic bone is shown in Fig. 4. Figure 5 shows the STL model of patient's skull obtained by the similar process.

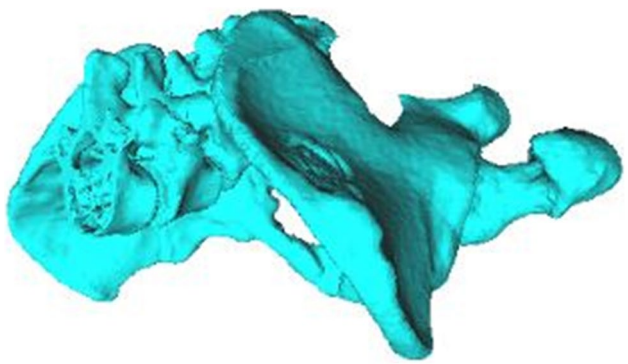

**Fig. 4** Preprocessed STL model of pelvic bone

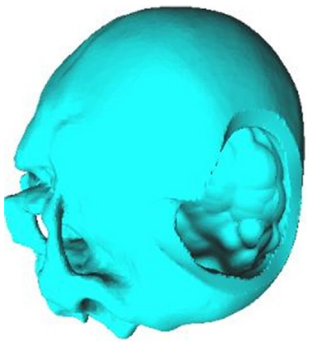

**Fig. 5** Preprocessed STL model of patient's skull

## 2.4 Design of patient-specific implants

The 3D models obtained from the DeVIDE software are faceted model, i.e. made up of triangular facets. The popular CAD software, such as SolidWorks, Creo/E, CATIA and NX UG can import these faceted files easily; however, in order to perform manipulation, they need to be converted into CAD format first through the lengthy and tricky process of reverse engineering. In order to avoid this lengthy conversion process, authors used Geomagic freeform plus software to design patient-specific implants. This software offers great flexibility of clay modelling, wherein virtual clay can be modified, remodelled and shaped like real tangible clay, allowing designers to create freeform features with great ease in comparison with conventional CAD software packages. The STL model of pelvic bone was imported into Geomagic freeform to design the implants. After importing the file, the software itself detects and auto corrects various errors that crept in during the importing process. After the rectifications, the STL file is converted into a CAD model, which can be modified now as clay modelling. After careful visualization of the CAD model of pelvic bone, three specific areas were identified which could be repaired using specific implants as shown in Fig. 6. For this purpose, three

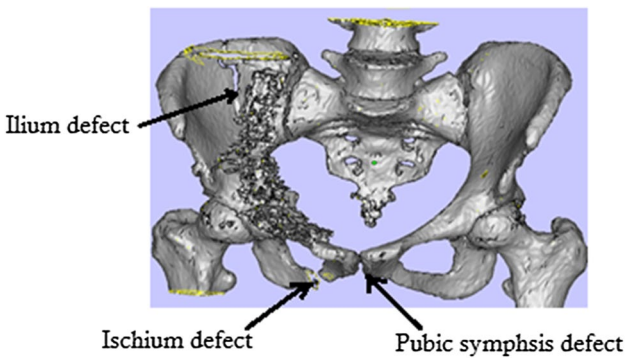


**Fig. 6** Defective areas on pelvic bone

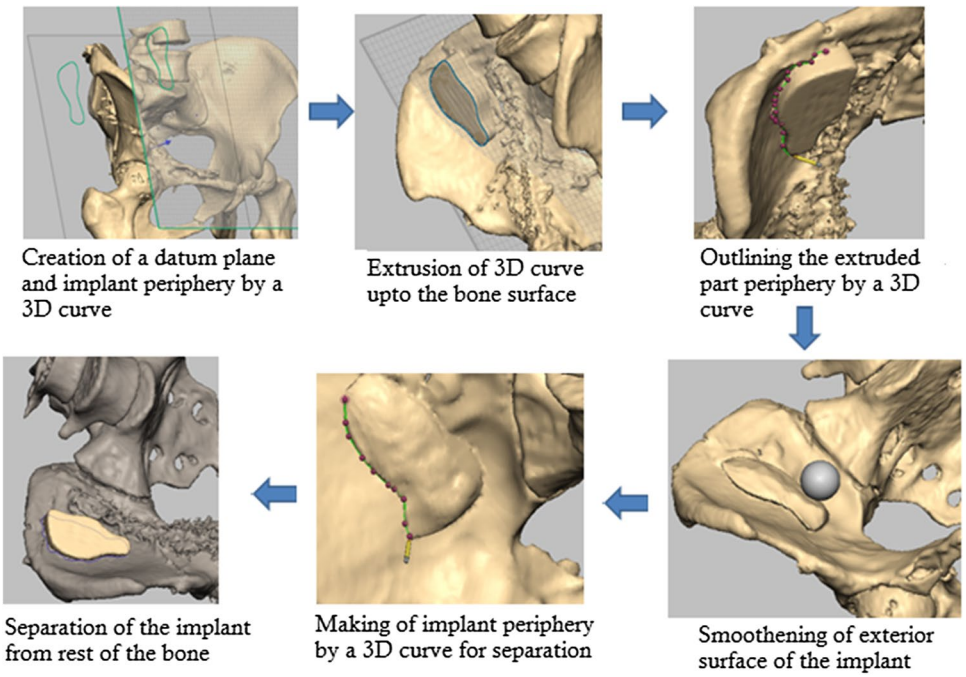


**Fig. 7** Process of designing ilium implant

implants, namely ilium, Pubic symphysis and Ischium implants were designed.

### 2.4.1 Ilium implant

Ilium implant was designed to repair the damaged right ilium surface as shown in Fig. 6. The implant must have a freeform surface which fits perfectly on the variable surface of the ilium portion. For this, a 3D curve was drawn around the periphery of the damaged area. A datum plane is introduced approximately 5 mm away from the pelvic bone perpendicular to the z-axis, and a 3D curve is projected on this datum plane. This projected curve is now extruded as continuous homogeneous virtual solid clay, with the datum plane as the base, towards the ilium surface, up to the first layer of clay encountered at the ilium surface, forming a continuous solid layer over the area enclosed by the first 3D surface. The top flat surface of the implant was modified conforming the surface of the parent bone leaving approximately 3 mm thickness of the implant. Process of designing ilium implant is shown in Fig. 7.

The designed implant is now separated and saved as STL file as shown in Fig. 8a. Similarly, other implants have been designed and saved as shown in Fig. 8b, c. Figure 9 shows the virtual model of pelvic bone with designed implants.

### 2.4.2 Cranium implant

Careful visual inspection of 3D model of the patient's cranium revealed that it was badly damaged on the 'frontal bone' and the 'parietal bone' of the right half of the

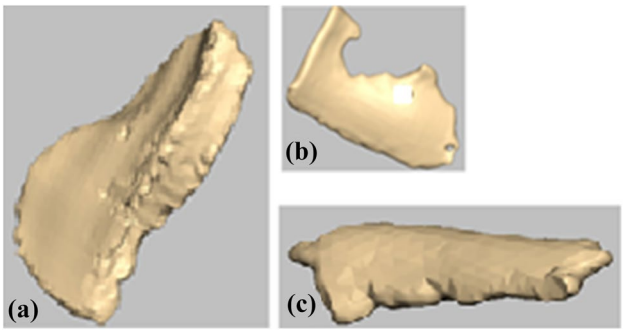


**Fig. 8** STL models of implants for pelvic bone **a** ilium, **b** pubic symphysis, **c** ischium

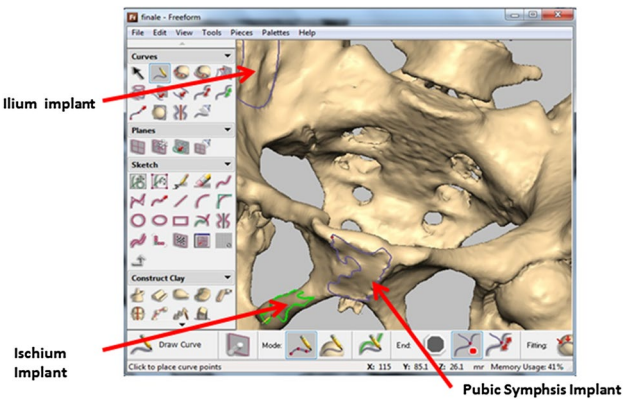


**Fig. 9** Virtual model of pelvic bone with implants

cranium. The junction of these two bones along with their respective portions was crushed into small pieces. Therefore, it was decided that these pieces be removed from both the patient's skull as well as from the reconstructed 3D model of the cranium. Hence, a gap was created extending from the frontal bone to the parietal bone. A cranial implant with thickness (approx. 5 mm) and shape matching with parent bone was designed in Geomagic freeform as discussed in the following paragraph to patch up this gap.

A number of points are selected in succession around the periphery of the gap. Then, a 3D curve is drawn to make a close loop curve. This closed loop serves as the boundary for the implant patch. For generating the patch, 'construct clay' tool is selected. A curved surface is generated within the volume enclosed by the 'cylinder' formed by two 3D curve rings which specify the upper and the lower boundaries of the roughly cylindrical patch. In this case, a series of 3D curved surfaces is generated between two 'rings' of 3D curves whose curvature can be controlled manually at the desired points by increasing or decreasing the radius as desired. The gap is filled using these curved surfaces. To ensure the symmetry of the shape of the cranium implant, 'mirror' option is used. Finally, the shapes are matched by removing or adding extra material using 'sculpt clay' and 'construct clay' tool. The outer boundary of the patch is smoothened and made tangential with the rest of the parent bone surface so that the implant fits well and matches the bone contour. Finally, the patch is separated from the skull using the 'separate' tool and exported as a separate STL file. Figure 10 shows virtual models of damaged skull as well as designed implant.

## 2.5 Finite element analysis of cranial implant

Finite element (FE) analysis of cranial implant for static loading conditions was carried out using Fusion 360 software (Student Edition, Autodesk, USA). For FE analysis, Polyamide PA 2200 was modelled using a linear, homogeneous and isotropic material model (Young's modulus (E) = 1700 MPa, Poisson's ratio (μ) = 0.4, ultimate tensile strength = 48 MPa [44]. A force of 200 N was applied vertically distributed on the top of the implant. To apply boundary condition, implant was fixed at four places, where actual implant would be screwed to skull. The CAD model was meshed into FUSION 360, and meshed model contained 66,186 nodes and 37,847 tetrahedron elements. Figure 11a, b shows the boundary condition and location of the load on the meshed implant.

Figure 12a, b shows the von Mises stress distribution and displacement of the cranial implant, respectively. Maximum stress observed is 6.02 MPa which is well below the allowable limit of material. Stress distribution is found uniform across implant body in range of 0–2.5 MPa and in range of 2.5–6.02 MPa near the areas of fixation. Maximum implant displacement in the direction of loading observed is 0.11 mm in the area directly under the loading. However, it is also well below the allowable limit of the material.

## 2.6 Additive manufacturing

The STL files of the designed implants and parent bones were now ready to be used as input to an AM machine. The final ready-to-use implants using additive manufacturing

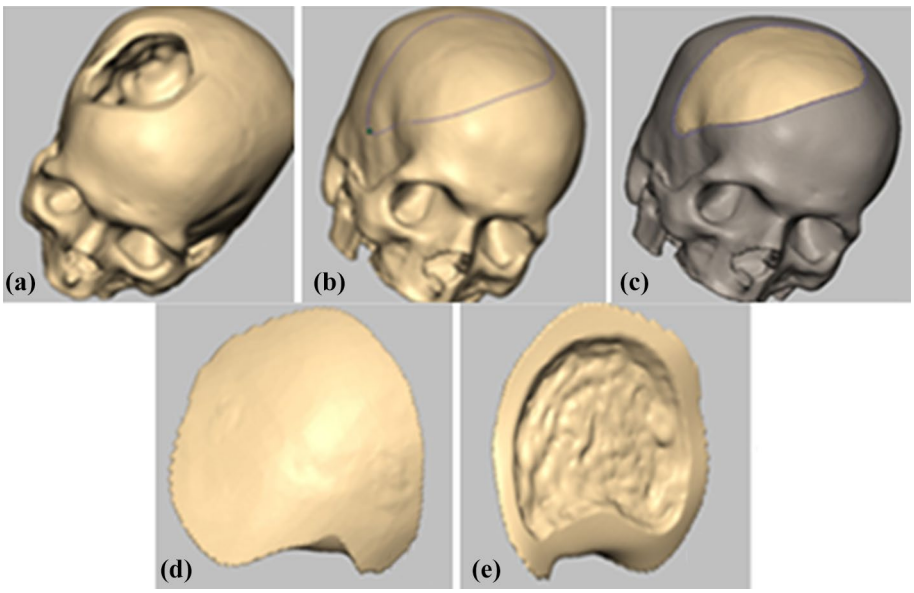


**Fig. 10** **a** CAD model of damaged skull, **b** 3D curve outline for implant, **c** implant separation from the skull, **d** separated implant outer view, **e** separated implant inner view

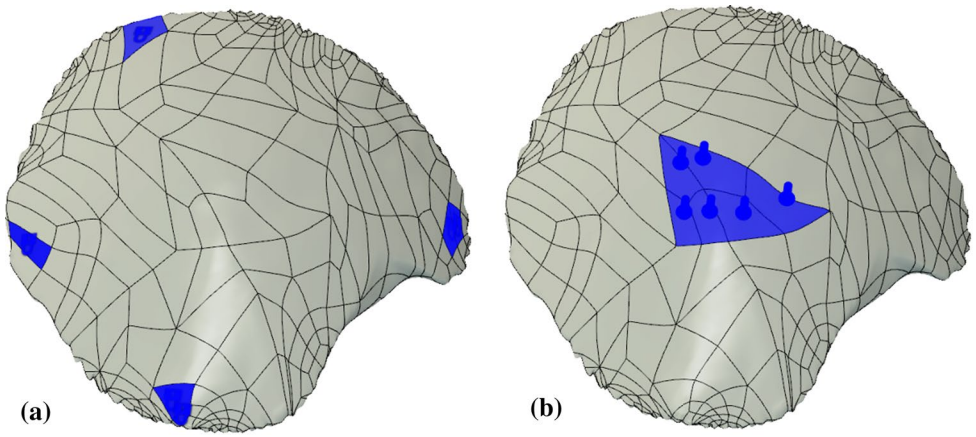


**Fig. 11** FE mesh of cranial implant model **a** boundary condition, **b** loading condition

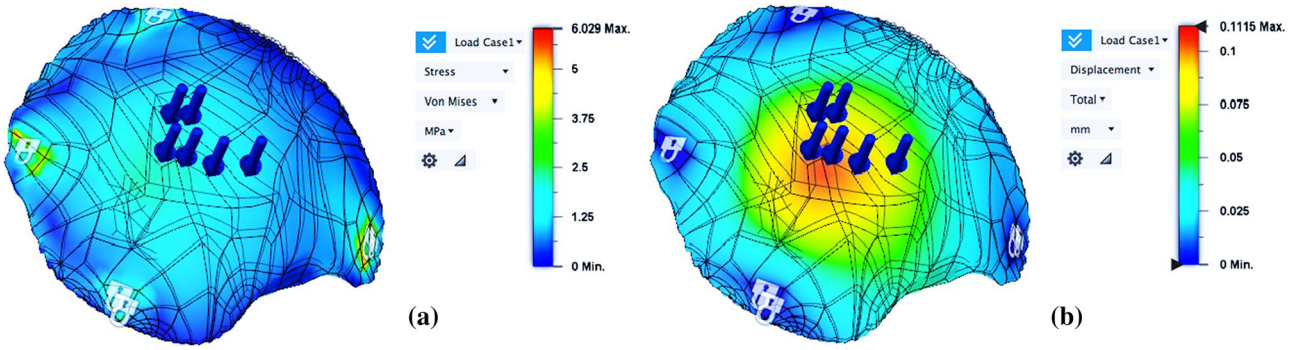


**Fig. 12** FE results of cranial implant **a** von Mises stress distribution, **b** deformation

may be obtained via two routes, (1) direct manufacturing of ready-to-use implants or (2) by using rapid tooling approach. In former case, AM machine must be capable of fabricating implants in bicompatible materials such as titanium alloy (Ti6Al4 V), stainless steel (316L), CrCoMo alloy, PEEK (poly-ether-ether-ketone), calcium phosphate/sulphate. AM processes like EBM (electron beam melting), SLM (selective laser melting) SLS (selective laser sintering), LENS (laser engineered net shaping), FDM (fused deposition modeling), 3D printer are used for this purpose. The latter case is suitable when a high-end AM machine capable of manufacturing metallic implant is not available. In this case, even a low-end AM machine can be used to manufacture a prototype of the implant. The prototype need not be made of biocompatible material. This prototype is then used to create a silicon or sand mould which is further used to cast end-use implant in biomaterials. Sand moulds are generally used to cast metallic implants, whereas silicon moulds may be used to produce polymeric implants like PMMA (polymethyl methacrylate) or may be used to produce wax expendable pattern to be used in investment casting of metallic implants [45].

In this study, authors have adopted the latter route. The STL files of the designed implants and parent bones have been loaded in Magics RP to fix any error in them using 'autocorrect' feature of the software. Nesting of various parts was also done in Magics RP. EOSINT P395, selective laser sintering machine by EOS GmbH, Germany, was used to fabricate the prototypes using PA2200 polyamide powder material. The following process parameters were used: laser type $CO_2$, laser power 50 W, scan speed 8 m/s, build temperature 176 °C and layer thickness 0.12 mm. The corrected STL files were sent to pre-processing software PSW 3.6 where the STL files were sliced in the layers of desired thickness. The machine was allowed to warm for 2 h before the desired temperature reached inside the build chamber. Manufacturing of all the parts took around 4 h. After about 8 h of cooling time, parts were removed from the chamber. The cranial implant fit perfectly on to skull model as shown in Fig. 13. Similarly, pelvic bone implants were also fitting properly on damaged areas on the pelvic bone model. These implants were used as pattern to cast end-use implants via rapid tooling approach. Figure 14 shows various pelvic implants with pelvic bone model.

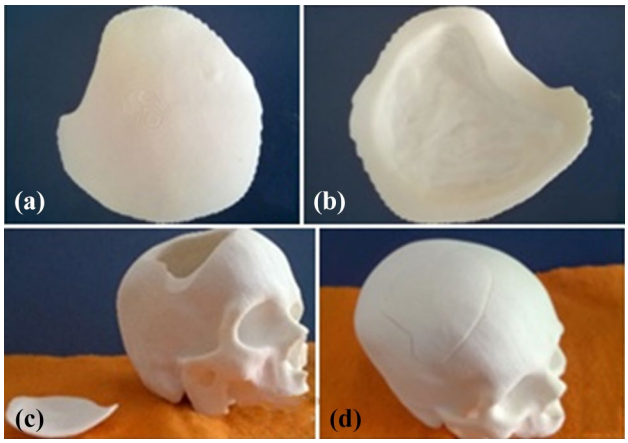


**Fig. 13** Polyamide (PA2200) prototypes fabricated on EOSINT P395 m/c **a** cranium implant outer view, **b** cranium implant inner view, **c** damaged skull and cranium implant, **d** cranium implant with skull

## 2.7 End-use implant by rapid tooling approach

The implant prototypes obtained from the EOSINT P395 process are used as a pattern to cast end-use implant. Due to the lack of adequate legal and ethical permissions, it was impossible to fit the implants inside the patient's body. So, it was decided to cast the implant in aluminium only. It is worth mentioning here that though metallic implants are less likely to fail after surgery, they may potentially damage the skull in case of second accident due to considerable difference in mechanical properties in comparison with bone. However, this problem can be minimized by providing an overlapping between implant and skull to increase the contact surface at interfacing [45]. In order to achieve a defect-free casting, the casting process was simulated using the E-Foundry [46], online learning resources in casting design and simulation by IIT Bombay. The results of the casting simulation process are shown in Fig. 15. The white and the yellow areas represent the hot spots (high-temperature zones) and the deep blue areas represent the cold spots (low-temperature zones) where rapid cooling may take place resulting in warping, cracks, cold shuts, etc. The aim of the simulation process was to obtain a uniform and relatively low temperature gradient by minimising the cold and the hot spot regions so as to obtain a defect-free casting. It was achieved by changing the orientation of the pattern as well as the positions of the gating system and the riser. After optimizing the casting parameters, a green sand mould was prepared for casting of cranium implant. Finally, molten aluminium was poured into mould cavity and allowed to cool down. Figure 16 shows the image of the aluminium casting of cranium implant.

## 2.8 Validation and sterilization of implants

After manufacturing, implant must be validated for mechanical, chemical and biological properties. Besides, they must be sterilized in order to ensure complete absence of all living organisms, such as virus, bacteria, yeasts and moulds before fitting inside the patient's body. Placement of unsterile implant may lead to nosocomial infection which can cause implant failure and serious illness to the patient [2, 34]. In this study, the final implant was not made in biocompatible titanium alloy, as the authors did not have necessary legal permissions to fit it inside the patient's body. However, the aluminium implant prototype was sterilized using autoclaving method. The implant prototype was kept

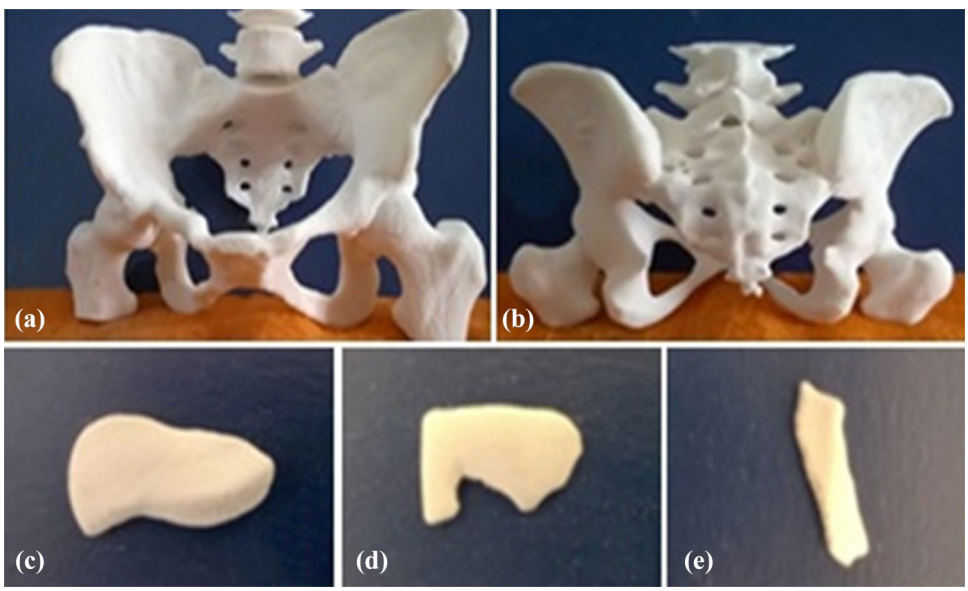


**Fig. 14** Polyamide (PA2200) prototypes fabricated on EOSINT P395 m/c (1:4 scale), **a** pelvic bone front view, **b** pelvic bone rear view, **c** ilium implant, **d** pubic symphysis implant, **e** ischium implant

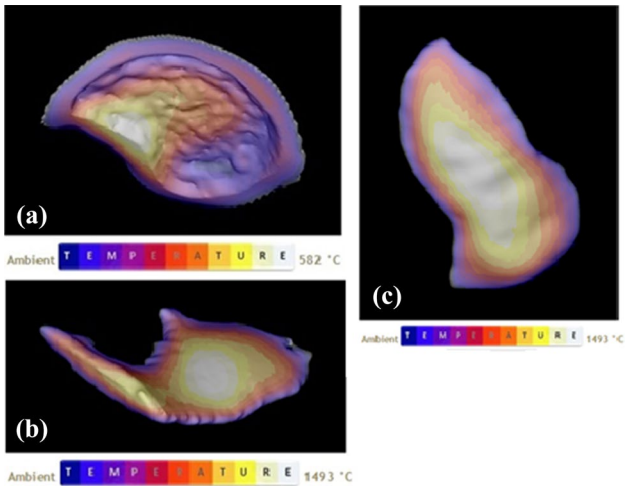


**Fig. 15** Casting simulation results **a** cranium implant, **b** pubic symphysis implant, **c** ilium implant

**Fig. 16** Aluminium green sand casting of cranium implant

in autoclave under controlled temperature and pressure condition (121 °C, 15 psi) for 30 min. These conditions are believed to be unsustainable for micro-organisms and spores. Chemical tape indicator was used to ensure that the sterilization condition reached inside the autoclave.

## 3 Surface roughness evaluation

Certain amount of roughness on implant surface is advisable for bone formation at the implant-bone interface. It promotes cell growth and enhances adherence characteristics of implant [47, 48]. A surface roughness value ranging between 1 and 100 µm results in higher degree of attachment of the cells to the implant. In the present case, the roughness value of the designed implants has been predicted by using an online facility. The STL files

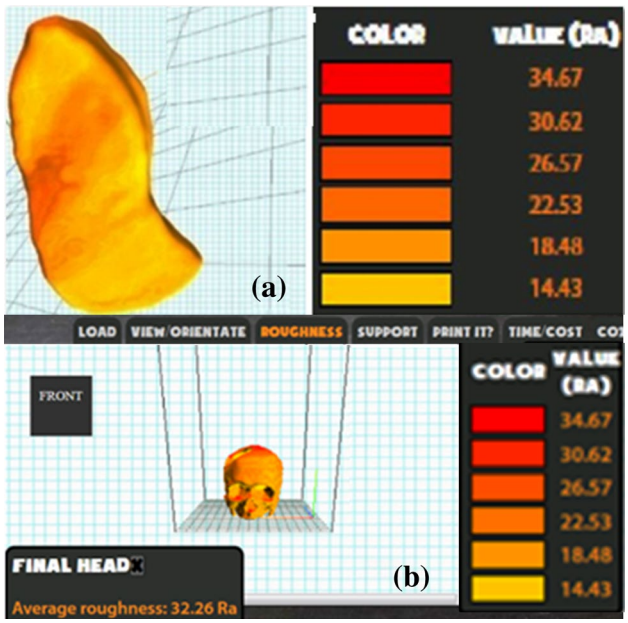


**Fig. 17** Roughness profile **a** ilium implant, **b** skull model

of implants were loaded into the software. The required parameters, such as AM machine type (EOSINT P395), standard build parameters, material used (PA2200), were fed into the software. The predicted $R_a$ values for various implants were found to be ranging between 14.4 and 34.67 µm. Roughness profile of the ilium implant and skull model is shown in Fig. 17.

## 4 Conclusions

This study describes the methodology to design and additively manufacture patient-specific biomodels and implants from CT scan data in relatively shorter period of time. FE study of cranium implant is successfully carried out using Fusion 360 software. Use of FEA tool for such complex problems overcomes the limitations of experimental and analytical approaches used for stress analysis. In this study, authors have manufactured only prototypes of implants; however, the same STL files can be used to obtain end-use implants in desired biomaterials by adopting direct or indirect route as discussed in the paper. At present, direct additive manufacturing of implants is costly due to costly high-end AM machines and software. Rapid tooling route (indirect manufacturing) is relatively cheaper than the direct route as low-end 3D printers can be used to fabricate prototypes. Use of open source software for designing of biomodels and implants will further reduce the cost of final implant. It can be summarized that a wise combination of free software, low-end 3D printers and rapid tooling approach paves the path for manufacturing of patient-specific economic

implants in shorter span of time. Additionally, additively manufactured patient-specific implant not only reduces the surgery and patient recovery time but also reduces the chances of implant failure in future.

**Acknowledgements** Authors gratefully acknowledge the help and support extended by the 3D Systems, USA, by providing access to trial versions of Geomagic Freeform and Geomagic Freeform Plus to design the patient-specific implants.

## Compliance with ethical standards

**Conflict of interest** On behalf of all authors, the corresponding author states that there is no conflict of interest.

## References

1. Bowers CA, McMullin JH, Brimley C, Etherington L, Siddiqi FA, Riva-Cambrin J (2015) Minimizing bone gaps when using custom pediatric cranial implants is associated with implant success. J Neurosurg Pediatr 16(4):439–444
2. Tuomi JT, Björkstrand RV, Pernu ML, Salmi MV, Huotilainen EI, Wolff JE, Vallittu PK, Mäkitie AA (2017) In vitro cytotoxicity and surface topography evaluation of additive manufacturing titanium implant materials. J Mater Sci–Mater Med 28(3):53
3. Ahn DG, Lee JY, Yang DY (2006) Rapid prototyping and reverse engineering application for orthopedic surgery planning. J Mech Sci Technol 20(01):19–128
4. Salmi M (2016) Possibilities of preoperative medical models made by 3D printing or additive manufacturing. J Med Eng. https://doi.org/10.1155/2016/6191526
5. Yap YL, Tan YSE, Tan HKJ, Peh ZK, Low XY, Yeong WY, Tan CSH, Laude A (2017) 3D printed bio-models for medical applications. Rapid Prototyp J 23(2):227–235
6. Thomas DJ, Azmi MM, Tehrani Z (2014) 3D additive manufacture of oral and maxillofacial surgical models for preoperative planning. Int J Adv Manuf Technol 71(9–12):1643–1651
7. Jelena M, Miroslav T (2007) Medical applications of rapid prototyping. Facta Univ Ser Mech Eng 5(01):79–85
8. Berce P, Chezan H and Balc N (2005) The application of rapid prototyping technologies for manufacturing the custom implants. In: Proceedings of the ESAFORM conference in Cluj-Napoca, Romania, pp 679–682
9. Sanadhya S, Vij N, Chaturvedi P, Tiwari S, Arora B, Modi YK (2015) Medical applications of additive manufacturing. Int J Sci Progress Res 12(1):11–17
10. Ngan E, Rebeyka I, Ross D et al (2006) The rapid prototyping of anatomic models in pulmonary atresia. J Thorac Cardiovasc Surg 132(02):264–269
11. Dhakshyani R, Nukman Y, Abu Osman AN, Vijay C (2011) Preliminary report: rapid prototyping models for dysplastic hip surgery. Central Eur J Med 6(03):266–270
12. Tuomi J, Paloheimo KS, Vehviläinen J, Björkstrand R, Salmi M, Huotilainen E, Kontio R, Rouse S, Gibson I, Mäkitie AA (2014) A novel classification and online platform for planning and documentation of medical applications of additive manufacturing. Surg Innov 21(6):553–559
13. Negi S, Dhiman S, Sharma RK (2014) Basics and applications of rapid prototyping medical models. Rapid Prototyp J 20(3):256–267
14. Modi YK, Agrawal S, de Beer DJ (2015) Direct generation of STL files from USGS DEM data for additive manufacturing of terrain models. Virtual Phys Prototyp 10(3):137–148
15. Agrawal S, de Beer DJ, Modi YK (2014) Conversion of a GIS surface data directly to a 3D STL part for terrain modeling. Rapid Prototyp J 20(5):422–430
16. Gibson I, Cheung LK, Chow SP et al (2006) The use of rapid prototyping to assist medical applications. Rapid Prototyp J 12(01):53–58
17. Ma D, Lin F, Chua CK (2001) Rapid prototyping applications in medicine Part 2: STL file generation and case studies. Int J Adv Manuf Technol 18:118–127
18. Winder J, Bibb R (2005) Medical rapid prototyping technologies: state of the art and current limitations for application in oral and maxillofacial surgery. J Oral Maxillofac Surg 63(07):1006–1015
19. Huotilainen E, Paloheimo M, Salmi M, Paloheimo KS, Björkstrand R, Tuomi J, Markkola A, Mäkitie A (2014) Imaging requirements for medical applications of additive manufacturing. Acta Radiol 55(1):78–85
20. Hieu LC, Zlatov N (2005) Medical rapid prototyping applications and methods. Assem Autom 25(4):284–292
21. Comaneanu RM, Tarcolea M, Vlasceanu D, Cotrut MC (2012) Virtual 3D reconstruction, diagnosis and surgical planning with Mimics software. Int J Nano Biomater 4(1):69–77
22. Singare S, Lian Q, Ping Wang W, Wang J, Liu Y, Li D, Lu B (2009) Rapid prototyping assisted surgery planning and custom implant design. Rapid Prototyp J 15(1):19–23
23. Mishra S (2016) Application of 3D printing in medicine. Indian Heart J 68:108–109
24. Sherekar RM, Pawar AN (2014) Application of biomodels for surgical planning by using rapid prototyping: a review and case studies. Int J Innov Res Adv Eng 1(6):263–271
25. Da Rosa EL, Oleskovicz CF, Aragao BN (2004) Rapid prototyping in maxillofacial surgery and traumatology: case report. Braz Dental J 15(03):243–247
26. Cohen A, Laviv A, Berman P, Nashef R, Abu TJ (2009) Mandibular reconstruction using stereolithographic 3-dimensional printing modeling technology. Oral Surg Oral Med Oral Pathol Oral Radiol Endodontol 108(05):661–666
27. Bertol LS, Junior WK, Silva FP, Kopp CA (2010) Medical design: direct metal laser sintering of Ti6Al4V. Mater Des 31(08):3982–3988
28. Ciocca L, Crescenzio FD, Fantini M, Scotti R (2009) CAD/CAM and rapid prototyped scaffold construction for bone regenerative medicine and surgical transfer of virtual planning: a pilot study. Comput Med Imaging Gr 33(01):58–62
29. Robiony M, Costa F, Bazzocchi M, Bandera C, Felice M (2007) Virtual reality surgical planning for maxillofacial distraction osteogenesis: the role of reverse engineering rapid prototyping and cooperative work. J Oral Maxillofac Surg 65(06):1198–1208
30. Chua CK, Jacob GGK, Mei T (1997) Interface between CAD and rapid prototyping systems Part 1: a study of existing interface. Int J Adv Manuf Technol 13(8):566–570
31. Chua CK, Jacob GGK, Mei T (1997) Interface between CAD and rapid prototyping systems Part 2: LMI–an improved interface. Int J Adv Manuf Technol 13(8):571–576
32. Bailey M (2005) Layered manufacturing for scientific visualization. Commun ACM 48(6):42–48
33. Chandramohan D, Marimuthu K (2011) Rapid prototyping/rapid tooling—a Overview and its applications in orthopaedics. Int J Adv Eng Technol 2(04):435–448
34. Park JH, Olivares-Navarrete R, Baier RE, Meyer AE, Tannenbaum R, Boyan BD, Schwartz Z (2012) Effect of cleaning and sterilization on titanium implant surface properties and cellular response. Acta Biomater 8(5):1966–1975

35. Delashaw J, Persing J (1996) Repair of cranial defects. In: Youmans JR (ed) Neurological surgery vol 4, pp 1853–1864
36. Salmi M, Tuomi J, Paloheimo KS, Björkstrand R, Paloheimo M, Salo J, Kontio R, Mesimäki K, Mäkitie AA (2012) Patient-specific reconstruction with 3D modeling and DMLS additive manufacturing. Rapid Prototyp J 18(3):209–214
37. Sanan A (1997) Repairing holes in the head: a history of cranioplasty. Neurosurgery 40:588–603
38. D'Urso P, Earwaker W, Barker T, Redmond M, Thompson R, Effeney D, Tomlinson F (2000) Custom cranioplasty using stereolithography and acrylic. Br J Plast Surg 53:200–204
39. Saringer W, Nobauer-Huhmann I, Knosp E (2002) Cranioplasty with individual carbon fibre reinforced polymere (CFRP)medical grade implants based on CAD/CAM technique. Acta Neurochir 144:1193–1203
40. Foustanos AP, Anagnostopoulos D, Kotsianos G, Rapidis AD (1983) Cranioplasty: a review of 10 cases. J Maxillofac Surg 11:83–86
41. Gladstone HB, McDermott MW, Cooke DD (1995) Implants for cranioplasty. Otolaryngol Clin North Am 28:381–400
42. Dujovny M, Aviles A, Agner C, Fernandez P, Charbel F (1997) Cranioplasty: cosmetic or therapeutic? Surg Neurol 47:238–241
43. Girod S, Teschner M, Schrell U, Kevekordes B, Girod B (2001) Computer-aided 3D simulation and prediction of craniofacial surgery: a new approach. J Cranio-Maxillofac Surg 29:156–158
44. Material data sheet PA2200: EOS GmbH. http://www.shapeways.com/topics/udesign/materials/white_strong_flexible/pa2200_material_data_sheet_12_08_en__.pdf. Accessed on September 14, 2018
45. Bonda DJ, Manjila S, Selman WR, Dean D (2015) The recent revolution in the design and manufacture of cranial implants: modern advancements and future directions. Neurosurgery 77(5):814–824
46. E-Foundry, online learning resources in casting design and simulation by IIT Bombay, http://efoundry.iitb.ac.in/Academy/index.jsp
47. Lacefield William R (2007) Materials characteristics of uncoated/ceramic-coated implant materials. Adv Dent Res 13:21–26
48. Albrektsson T, Berglundh T, Lindhe J (2003) Osseointegration: historic background and current concepts. In: Clinical periodontology and implant dentistry, 4th ed., Blackwell Munksgaard, Oxford, pp 809–820